Parameters of the energy spectrum for holes in CuInSe$_2$

P.M. Gorley[1], I.V. Prokopenko[2], O.O. Galochkina[1], P.P. Horley[1,3], Yu.V. Vorobiev[4], J. González-Hernández[5]
[1]*Yu. Fedkovych Chernivtsi National University, 2, Kotsyubynsky str., 58012 Chernivtsi, Ukraine,*
phone: +38 (03722) 46-877, e-mail: semicon-dpt@chnu.edu.ua
[2]*V. Lashkaryov Institute of Semiconductor Physics, NAS of Ukraine, 41, prospect Nauky, 03028 Kyiv, Ukraine*
[3]*Centro de Física das Interacções Fundamentais (CFIF), Instituto Superior Técnico,*
Avenida Rovisco Pais, 1049-001 Lisboa, Portugal
[4]*CINVESTAV-IPN Unidad Querétaro, Libramiento Norponiente 2000, Fracc. Real Juriquilla,*
76230 Querétaro, México
[5]*CIMAV, Miguel de Cervantes 120, Complejo Industrial Chihuahua, 31109 Chihuahua, México*

Abstract. This paper reports the coefficients $C_{A,B}$ for the k-linear term in dispersion relation $E(k)$ for holes of the upper valence bands Γ_6^- and Γ_7^+ in p-CuInSe$_2$ crystals. We also obtained the tensor components for the carrier effective masses $m_{\perp,\parallel}^{A,B,C}$ in all three valence sub-bands of the model semiconductor. It was shown that the energy spectrum parameters for holes in CuInSe$_2$ allow successful explanation for the anisotropy of tensor components describing the interband light absorption coefficient and the published data for the temperature variation of the Hall coefficient, total Hall mobility and thermal voltage within the temperature range 100 K $\leq T \leq$ 350 K.

Keywords: chalcopyrite structure, CuInSe$_2$, non-parabolic dispersion relation, components of the effective mass tensor, kinetic coefficient, light absorption coefficient.

1. Introduction

Direct-band chalcopyrite compound CuInSe$_2$ belongs to A^{I}B^{II}C$^{VI}_2$ semiconductors that are considered as analogs to A^{II}B^{VI} binary systems. Due to their high absorption coefficient [1] (about $(3…6)\cdot10^7$m^{-1}) these materials are very promising for the efficient photovoltaic device applications [2]. In general, CuInSe$_2$ crystals are studied in deeper detail comparing with the other A^{I}B^{II}C$^{VI}_2$ compounds (*e.g.*, [3-5]). However, the exact nature of some of their properties is not clearly revealed yet. In particular, it concerns the fundamental parameters characterizing the valence band structure. According to the results of the theoretical calculations [6, 7], the band structure of the bulk A^{I}B^{II}C$^{VI}_2$ semiconductors in the center of the Brillouin zone obeys anisotropic non-parabolic dispersion relation $E(\mathbf{k})$ including a **k**-linear term. To the best of the authors' knowledge, the numerical values of the coefficients C describing the aforementioned term are not determined yet for p-CuInSe$_2$ crystals, while they are known for the A^{II}B^{VI} materials p-CdS, p-CdSe and p-ZnO. Moreover, only three out of six components of the hole effective masses

for p-CuInSe$_2$ were determined so far from the optical studies [8]: those for spin-split band holes ($m_{sh}/m_0 \approx 0.085$), heavy ($m_{hh}/m_0 \approx 0.71$) and light holes ($m_{hl}/m_0 \approx 0.092$).

Our previous research [9] considered non-parabolicity of the dispersion relation $E(\mathbf{k})$ for the holes in chalcopyrite-structure crystals under non-degenerate statistics of the electron gas, deriving the analytical expressions allowing to calculate the temperature and concentration dependences of tensor components for the thermal voltage, Hall coefficient and carrier mobility. Carrier scattering by crystalline lattice defects was considered in the approximation of time relaxation. For the upper valence sub-bands Γ_6^- and Γ_7^+ of p-CuInSe$_2$, we estimated the coefficients $C_{\Gamma_6^-, \Gamma_7^+}$ characterizing the contribution of **k**-linear term into $E(\mathbf{k})$. The results of further calculations agreed well with the experimental temperature dependences of the Hall coefficient and total Hall carrier mobility.

To improve the approach used in [9], we suggest also to account for the symmetry relations binding the tensor components of the inverse effective masses for

the holes $(m_{\Gamma_6^-,\Gamma_7^+,\Gamma_7})^{-1}$ in chalcopyrite (wurtzite) crystals [10-12]. This methodological improvement would change the values of $C_{\Gamma_6^-,\Gamma_7^+}$ obtained in [9], leading to more exact results concerning the influence of k-linear term of $E(\mathbf{k})$ on the values and temperature behavior of the kinetic coefficients in p-CuInSe$_2$. Moreover, proper accounting of the symmetry for the components $(m_{\Gamma_6^-,\Gamma_7^+,\Gamma_7})^{-1}$ allows to get an accurate magnitude estimation for all the inverse effective mass components describing the holes in three valence sub-bands of the material studied. Fitting the theoretical calculations to the experimental data on temperature dependences for the Hall coefficient, Hall mobility and thermal voltage in p-CuInSe$_2$ crystals allowed to improve precision in determining $C_{\Gamma_6^-,\Gamma_7^+}$ coefficients.

We have also shown that non-parabolicity contribution to $E(\mathbf{k})$ in the total Hall mobility decreased from about 50 % ($T = 100$ K) to 17 % ($T = 300$ K), enhancing the previously reported data of ≈ 20 % and ≈ 10 %, respectively [9].

2. Theory

Schematic depiction of the valence band diagram [4, 13] for p-CuInSe$_2$ around the center of the Brillouin zone is shown in Fig. 1.

The dispersion relation for the carriers populating the valence bands Γ_6^-, Γ_7^+ and Γ_7 (taking into account spin-orbital interaction) can be written in the following form [7]:

$$E_{\Gamma_6^-,\Gamma_7^+}(\vec{k}) = E_0^{A,B} + \frac{\hbar^2}{2m_\perp^{A,B}} \times$$
$$\times (k_\perp \mp m_\perp^{A,B} \cdot C_{A,B}/\hbar^2)^2 + \frac{\hbar^2 k_\parallel^2}{2m_\parallel^{A,B}}, \quad (1)$$
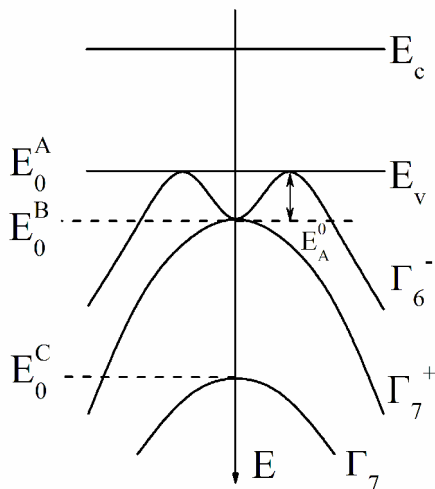

Fig. 1. Band diagram for p-CuInSe$_2$; the designations are explained in the text.

$$E_{\Gamma_7}(\vec{k}) = E_0^C + \frac{\hbar^2}{2}\left(\frac{k_\perp^2}{m_\perp^C} + \frac{k_\parallel^2}{m_\parallel^C}\right), \quad (2)$$

with transversal $k_\perp = (k_x^2 + k_y^2)^{1/2}$ and longitudinal $k_\parallel = k_z$ components of the wave vector $\mathbf{k}$ for $m_\perp^{A,B,C}$ and $m_\parallel^{A,B,C}$ effective mass tensors describing the holes in the sub-bands Γ_6^- (index A), Γ_7^+ (index B) and Γ_7 (index C) regarding the high-symmetry axis of the crystal. The coefficients $C_{A,B}$ characterize the deviation from parabolicity in the dispersion relation $E(\mathbf{k})$ for the corresponding valence sub-bands. $E_0^{A,B,C}$ in (1) and (2) describe the position of their extrema.

As the dispersion relation (1) is characteristic for the semiconductors with chalcopyrite or wurtzite structure of [14-17], it is natural to assume that the components of the effective mass tensors for p-CuInSe$_2$ would also satisfy the relations obtained for wurtzite crystals [11, 12]:

$$\frac{m}{m_\parallel^{B,C}} - \frac{m}{m_\parallel^A} = \Delta\left(\frac{m}{m_\perp^{B,C}} - \frac{m}{m_\perp^A}\right),$$

$$\frac{m}{m_\perp^A} - \frac{m}{m_\parallel^A} = \frac{(g-r)(2+\Delta_1)}{1+C_2+C_3},$$

$$\frac{m}{m_{\parallel,\perp}^B} - \frac{m}{m_{\parallel,\perp}^A} = C_1\left(\frac{m}{m_{\parallel,\perp}^C} - \frac{m}{m_{\parallel,\perp}^A}\right),$$

$$\frac{m}{m_\perp^C} - \frac{m}{m_\parallel^C} = C_2\left(\frac{m}{m_\perp^A} - \frac{m}{m_\parallel^A}\right),$$

$$\frac{m}{m_\perp^B} - \frac{m}{m_\parallel^B} = C_3\left(\frac{m}{m_\perp^A} - \frac{m}{m_\parallel^A}\right). \quad (3)$$

Here g, r, s, t denote $\hbar^2/2m$-normalized ($\hbar$ is Planck's constant and m is the free electron mass) matrix elements for the interband interaction operators [12], with adjustment parameters

$$\Delta = \frac{t-r}{s-g}, \quad \Delta_1 = \frac{s-t}{g-r}, \quad C_2 = (1-q^2)\cdot(C_1+\Delta_1),$$

$$C_3 = (1-q^2)\cdot(1+\Delta_1 C_1). \quad (4)$$

The coefficient

$$C_1 = q^2/(1-q^2) \quad (5)$$

with

$$q^2 = \frac{1}{2}\left[1 - \frac{x}{\sqrt{x^2+8/9}}\right] \quad (6)$$

depends on the energy split $x = \Delta_{cr}/\Delta_{so} - 1/3$ caused by the crystalline field Δ_{cr} and spin-orbital interaction Δ_{so} [10]. It is important that the mc-normalized (m is the electron mass and c is the speed of light) matrix elements for the optical transitions from B/C valence

sub-bands to the conduction band [10] also depends on q^2

$$M_\parallel^B = 2M_\perp^C = q^2, \quad M_\parallel^C = 2M_\perp^B = 1 - q^2, \qquad (7)$$

while for the A-band $M_\parallel^A = 0$, $M_\perp^A = 0.5$.

The experimental values $\Delta_{cr} = 0.006\,\mathrm{eV}$ and $\Delta_{so} = 0.233\,\mathrm{eV}$ [18] lead to $C_1 \approx 1.9 > 1$, proving that for p-CuInSe$_2$ (and also CdSe, ZnSe) the components of the effective mass tensor for holes in the valence sub-bands would satisfy the condition [12]:

$$m_\parallel^B < m_\parallel^C < m_\parallel^A, \quad m_\perp^A < m_\perp^C < m_\perp^B. \qquad (8)$$

It is important that for $C_1 < 1$ (which is valid for CdS, ZnS, ZnO and GaN), the components of symmetry for the effective mass tensor are [10-12]

$$m_\parallel^C < m_\parallel^B < m_\parallel^A, \quad m_\perp^A < m_\perp^B < m_\perp^C. \qquad (9)$$

Comparison of (8) and (9) shows that changing $C_1 > 1$ for $C_1 < 1$ will result in swapping of the valence sub-bands B and C.

Formulas (5) and (7) yield a proportion $C_1 = M_\parallel^B / M_\parallel^C = M_\perp^C / M_\perp^B$ saying that the coefficient C_1 depends on the ratio of matrix elements for the optical transitions (with the same polarization) from the bands B/C into conduction band. Therefore, one can assume that C_1 should contribute somehow to the anisotropy of the light absorption coefficient $\alpha_\parallel / \alpha_\perp$ (with parallel and perpendicular subscripts denoting light polarization regarding the main optical axis of the crystal).

3. Results and discussion

Using the symmetry relations (3) one can show that for the present experimental effective mass values describing the holes of p-CuInSe$_2$ [8] the inequalities (8) would be valid for these two particular cases (within parameters with the precision of experimental measurements):

Case D$_1$: $\dfrac{m_\parallel^A}{m} = 0.091$, $\dfrac{m_\parallel^B}{m} = 0.074$, $\dfrac{m_\parallel^C}{m} = 0.081$,

$\dfrac{m_\perp^A}{m} = 0.087$, $\dfrac{m_\perp^B}{m} = 0.73$, $\dfrac{m_\perp^C}{m} = 0.162$;   (10)

Case D$_2$: $\dfrac{m_\parallel^A}{m} = 0.71$, $\dfrac{m_\parallel^B}{m} = 0.165$, $\dfrac{m_\parallel^C}{m} = 0.260$,

$\dfrac{m_\perp^A}{m} = 0.078$, $\dfrac{m_\perp^B}{m} = 0.092$, $\dfrac{m_\perp^C}{m} = 0.085$.   (11)

Table 1 presents the anisotropy coefficients for effective masses of holes $K_{m\perp,\parallel}^{A,B,C} = \dfrac{m_\parallel^{A,B,C}}{m_\perp^{A,B,C}}$. We calculated the data both for p-CuInSe$_2$ crystals and their A^{II}B^{VI} analogs using the experimental mass values for CdSe, CdS [10] and ZnO [14].

Table 1. Anisotropy coefficients for hole effective masses in p-CuInSe$_2$ and A^{II}B^{VI} analogs.

Material	K_m^A		K_m^B	K_m^C	E_g, eV	C_1
p-CIS	Case C1	1.05	0.10	0.50	$1.010^{[22]}$	1.90
	Case C2	9.10	1.79	3.06		
p-CdSe	2.66		0.53	0.91	$1.756^{[23]}$	1.65
p-CdS	4.70		0.76	0.48	$2.485^{[23]}$	0.73
p-ZnO	5.07		3.76	0.24	$3.370^{[23]}$	0.035

As one can see, for the case C$_1$ (10) with increasing band gap E_g (parameter C_1 decreases) the anisotropy coefficient for effective masses of the holes populating A and B valence bands also increases. At the same time, the coefficient for the C-band decreases for all the studied materials except for CdSe. Effective mass components calculated for the case D$_2$ (11) for CuInSe$_2$ violate this regularity for A and B-bands, to the contrary restoring it for the C-band.

To define which of the cases D$_1$ or D$_2$ is correct for p-CuInSe$_2$, we used analytical expressions from [9] to calculate temperature behavior of the tensors describing the specific conductivity, Hall mobility and thermal voltage. To define the fixed $m_{\perp,\parallel}^{A,B,C}$, the coefficients $C_{A,B}$ in the dispersion relation (1) were considered as parameters and adjusted to achieve the best fitting of the calculated data to the experimental temperature curves for the kinetic coefficients. The numerical values of $C_{A,B}$ for p-CuInSe$_2$ and A^{II}B^{VI} are given in Table 2.

It is noteworthy that for all the studied compounds we achieved an essentially linear dependence $C_B = 4.65 \cdot 10^{-2}(4.15 - E_g)$ eV·Å   (Fig. 2,   line 2), allowing to assume the linearity of $C_A = \psi(E_g)$ as well. To obtain the latter (Fig. 2, line 1) the values of C_A for CdSe and CdS should be used in the place of those from [15], which will allow to get the refined coefficients (Table 2). Validity of $C_{A,B} = k_{A,B}(E_0 - E_g)$ dependence for various wurtzite and chalcopyrite crystals makes it possible to estimate the limit values of $C_{A,B}$ coefficients for the case $E_g \to 0$, yielding $C_A^{max} = 0.263$ eV·Å   and $C_B^{max} = 0.193$ eV·Å, respectively. On the other hand, for semiconductor with the considered crystalline structure and a bandgap of $E_g \geq 4.15\,\mathrm{eV}$, the contribution of **k**-linear term into $E(\mathbf{k})$ should be negligibly small. Due to this fact, for example, the bandgap of BeO is not determined yet exactly, so that the publication [19] usually mentions the data in a wide range of 7.8-10.6 eV. The fact that the linear dependence $C_{A,B} = k_{A,B}(E_0 - E_g)$ holds for p-CuInSe$_2$ crystals and their A^{II}B^{VI} analogs suggests that the obtained $C_{A,B}$ coefficients are determined correctly and reliably.
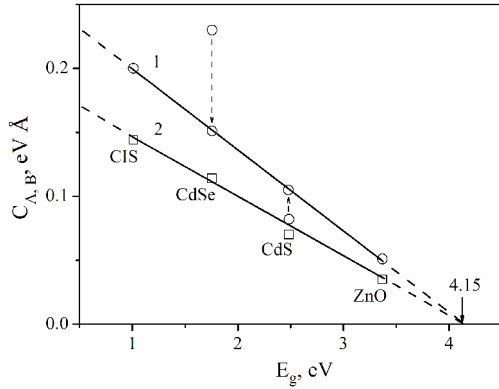
Fig. 2. Dependence of C_A (line 1) and C_B (line 2) coefficients from (1) on the bandgap of p-CuInSe$_2$ crystals and their A^{II}B^{VI} analogs. The arrows mark the refined C_A for CdSe and CdS, which fits the linear dependence $C_A = 6.34 \cdot 10^{-2} \cdot (4.15 - E_g)$ eV·Å.
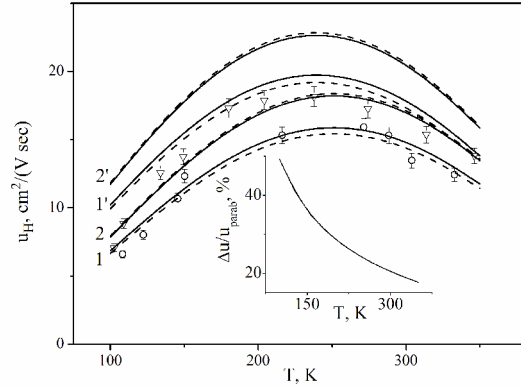

Fig. 3. Temperature dependence of the total Hall mobility for holes in p-CuInSe$_2$. The curve numbering is discussed in the text. Error bars illustrate precision of the experiment.

Table 2. Coefficients $C_{A,B}$ for p-CuInSe$_2$ and their A^{II}B^{VI} analogs (eV·Å units).

Material	p-CuInSe$_2$ our data	p-CdSe data [15] / refined	p-CdS data [15] / refined	p-ZnO data from [15]
C_A	0.200	0.230/0.150	0.082/0.105	0.051
C_B	0.144	0.114	0.070	0.035

Concerning the temperature behavior of kinetic coefficients in p-CuInSe$_2$, our calculations show that the carrier contribution to the valence band Γ_7 is negligibly small in comparison with that of the holes populating Γ_6^- and Γ_7^+ bands. Let us consider the system with a single acceptor level formed by interstitial selenium atoms [20] with the concentration $N_a \approx 4.0 \times 10^{18}$ cm^{-3} and depth $E_V + 0.019 \pm 0.002$ eV correlating with the data from [21]. We performed calculations for this system by using carrier effective masses calculated for either of C$_1$ and C$_2$ cases (10), (11). The results revealed good agreement between theoretical and experimental [9] results concerning the temperature dependence of the Hall coefficient $R = f(1/T)$. The calculated thermal voltage degenerates into a scalar value, fitting the experimental data [9] within the precision limits of the experimental measurements.

Solid and dashed curves in Figure 3 present calculation results for the cases D$_1$ and D$_2$, respectively. The curves designated numbers with primes *1′, 2′* were obtained for $C_{A,B} \neq 0$. The temperature dependence of the total Hall mobility for holes $u_H(T)$ in p-CuInSe$_2$ crystals for the different experimental results are shown with circles (data [24]) and triangles (data [25]). Comparing the results presented by curves *1* and *1′* with *2* and *2′*, one can see that for the case when non-parabolicity of $E(\mathbf{k})$ is neglected, one obtains the excess

mobility and markedly different shape of the curve $u_H(T)$. For $C_{A,B} \neq 0$, the calculated and experimental curves for $u_H(T)$ fit each other well for the temperatures $170 \text{ K} \leq T \leq 350 \text{ K}$. The existing mismatch between theory and experiment for $u_H(T)$ in p-CuInSe$_2$ crystals under $T < 150$ K may stem from neglecting the hopping scattering, which becomes quite significant at these temperatures [20]. Under the temperature increase from 100 to 300 K the contribution of non-parabolicity into the hole mobility was calculated using the masses (10), (11) and the experimental data [24, 25]. We observed a decrease of aforementioned contribution for approximately 33 percents (from $\approx$50 % at 100 K to $\approx$ 17 % at 300 K), which is illustrated at the inset to Fig. 2 for the parameter $\Delta u / u \equiv (u_H(C_{A,B} \neq 0) / u_H(C_{A,B} = 0) - 1) \cdot 100\%$. The resulting difference between the values of the total mobility calculated using D$_1$ and D$_2$ effective hole masses for p-CuInSe$_2$ (the corresponding solid and dashed curves in Fig. 2) are within the experimental precision. Due to this, it is hard to say which set of $m_{\perp,\parallel}^{A,B,C}$ (D$_1$ or D$_2$) is preferable for the description of temperature variation of the kinetic coefficients in p-CuInSe$_2$.

To solve this problem, we used the experimental spectrum [26] for imaginary part k_i of the refraction coefficient n of CuInSe$_2$, measured for different polarizations $i = \perp, \parallel$ regarding the main crystalline axis and the incident light wave with a wavelength λ. The knowledge of the latter allowed us to apply the formula [26]

$$\alpha_i = 4\pi k_i / \lambda \qquad (12)$$

to determine the components of absorption coefficient α_i. On the other hand [20], the expression for α_i at the fundamental absorption edge in semiconductor material can be written as:

$$n \cdot \alpha_i \cdot \hbar\omega = A_i \sqrt{\hbar\omega - E_g} , \qquad (13)$$

where

$$A_i = \frac{c \cdot m^{3/2}}{6\pi V \varepsilon_0} \cdot \frac{e^2}{\hbar^2} \cdot \sum_{n=A,B,C} (2m_{ir}^n / m)^{3/2} (M_i^n)^2 . \qquad (14)$$

Here n is the carrier concentration, $\hbar\omega$ is the photon energy, $\dfrac{1}{m_{ir}^n} = \dfrac{1}{m_i^e} + \dfrac{1}{m_i^n}$ describes the i-th component of the reduced mass of electron-hole pair (m_i^e is the i-th component of effective mass tensor for conduction band electrons), M_i^n are matrix elements for optical transitions (6), V is the volume of the crystal, e is the elementary charge, and ε_0 is the absolute dielectric permittivity.

Calculating D_1 and D_2 effective masses for the holes (Table 1) and using electron effective masses (for CuInSe$_2$ – $m_\perp / m = 0.10$, $m_\parallel / m = 0.11$ [24], for CdSe – $m_\perp / m = 0.13$, $m_\parallel / m = 0.14$ [15], for CdS – $m_\perp / m = 0.21$, $m_\parallel / m = 0.22$ [15] and for ZnO – $m_\perp / m = 0.30$, $m_\parallel / m = 0.31$ [27]), we calculated dimensionless variable $A_{\perp,\parallel}^* \equiv \dfrac{6\pi V \varepsilon_0}{c \cdot m^{3/2}} \cdot \left(\dfrac{e}{\hbar}\right)^2 \cdot A_{\perp,\parallel}$ as a function of semiconductor bandgap E_g (Fig. 4).

As it can be seen from the figure, the dependence $A_{\perp,\parallel}^* = f(E_g)$ can be quite well described within experimental precision for $m_{\perp,\parallel}^{A,B,C}$, Δ_{cr} and Δ_{so} as

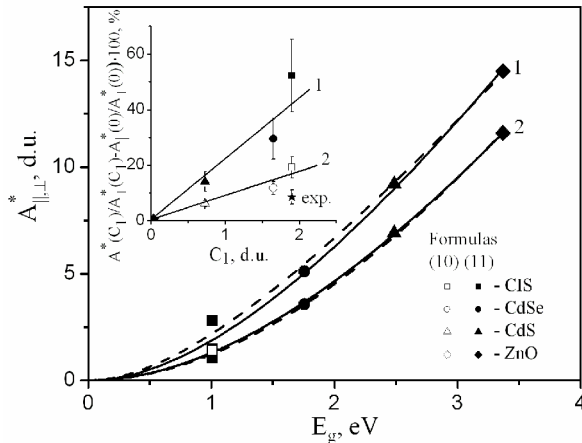$$A_{\perp,\parallel}^* = \beta_{\perp,\parallel} E_g^2 / (E_g + \gamma_{\perp,\parallel}) . \qquad (15)$$

Fig. 4. $A_\parallel^*$ (*1*) and $A_\perp^*$ (*2*) coefficients as the function of E_g for p-CuInSe$_2$ and its A^{II}B^{VI} analogs (solid and dashed curves correspond to D_1 and D_2 hole masses, respectively). The inset shows the ratio $A_\parallel^* / A_\perp^*$ with variation of the parameter C_1: line *1* – for the masses (11) and line *2* – for the masses (10). The error bars illustrate dispersion of the theoretical values obtained for the different experimental data. The asterisk denotes the experimental result for p-CuInSe$_2$ [22].

For further calculations, one should use the following values for $\beta_{\perp,\parallel}$ (in eV^{-1}) and $\gamma_{\perp,\parallel}$ (in eV):

for the case D$_1$ (10) –

$$\beta_\perp = 11.65, \quad \gamma_\perp = 8.03, \quad \beta_\parallel = 9.83, \quad \gamma_\parallel = 4.28; \qquad (16)$$

for the case D$_2$ (11) –

$$\beta_\perp = 14.20, \quad \gamma_\perp = 10.47, \quad \beta_\parallel = 7.22, \quad \gamma_\parallel = 2.32 . \qquad (17)$$

As it follows from the latter formulas, the components of absorption coefficient are bounded with the proportion $\alpha_\parallel / \alpha_\perp = k_\parallel / k_\perp = A_\parallel^* / A_\perp^*$. According to [26], the experimental ratio $k_\parallel / k_\perp$ for the case of the fundamental absorption in CuInSe$_2$ crystals varies within the range $1.05 - 1.10$. The same ratio, calculated according from (15) using (16) and (17), would yield the values 1.44 and 1.75 for the cases D$_1$ and D$_2$, respectively. Therefore, the best fit of theoretical curves to the experimental data regarding $\alpha_\parallel / \alpha_\perp$ ratio can be attained by using the hole effective masses according to the case D$_1$ (formula (10)).

It was experimentally proven [28, 29] that in quasi-cubic model approximation for the crystals with chalcopyrite structure [30] illuminated by light wave with the polarization vector perpendicular to the main optical axis of the crystal, the ratio of intensity peak in electro-reflection spectra ($I_\parallel$ and $I_\perp$) obeys the following expressions:

$$\frac{I_\parallel}{I_\perp}\bigg|_A = 0, \qquad \frac{I_\parallel}{I_\perp}\bigg|_{B,C} = 9 \cdot (2/3 - E_\mp / \Delta_{so})^2 \qquad (18)$$

with

$$E_\mp = 0.5 \cdot \left(\Delta_{so} + \Delta_{cr} \mp \sqrt{(\Delta_{so} + \Delta_{cr})^2 - \frac{8}{3}\Delta_{so}\Delta_{cr}} \right) . (19)$$

The discussed peaks correspond to electron transitions from the valence to conduction band in the crystals A^{II}B^{IV}C$^V_2$. It is worth noting that for the limit case $\Delta_{so} \to 0$ the ratio E_- / Δ_{so} tends to 2/3. Taking into account (5), (6), one can show that for the crystals with $C_1 > 1$

$$\frac{I_\parallel}{I_\perp}\bigg|_C = 2 \cdot C_1, \qquad \frac{I_\parallel}{I_\perp}\bigg|_B = 2 / C_1 . \qquad (20)$$

For the case $C_1 < 1$, the subscripts "B" and "C" should be swapped in (20).

In this way, one can treat the ratio $\alpha_\parallel / \alpha_\perp = A_\parallel / A_\perp$ as a function of the parameter C_1 for the crystals with chalcopyrite or wurtzite structure. The inset to Fig. 4 proves that the dependence $\left(A_\parallel^* / A_\perp^* - A_\parallel^*(0) / A_\perp^*(0)\right) \cdot 100\%$ is linear and equal to $(8 \pm 1) \cdot C_1$ or $(21 \pm 2) \cdot C_1$ for the hole masses calculated for the cases D$_1$ and D$_2$. Experimental data on this ratio for p-CuInSe$_2$ (shown as the asterisk in the inset to Fig. 4) fits better to the case when the effective mass estimations are done with the formula (10). The obtained correlations

between $A_{\perp,\parallel}$ and their ratio for the different wurtzite and chalcopyrite crystals (*e.g.*, $CuInSe_2$, CdSe, CdS and ZnO, see Fig. 4) suggests that the most accurate description of the effective mass tensor for p-$CuInSe_2$ is that provided with the formulas (10).

4. Conclusions

We show that p-$CuInSe_2$ crystals with the components of hole effective mass tensor obeying the symmetry relations (3) is characterized with two sets of $m_{\perp,\parallel}^{A,B,C}$, describing temperature dependence of the total conductivity, Hall coefficient and thermal voltage within experimental precision. For the upper valence sub-bands Γ_6^- and Γ_7^+, we have estimated the coefficients $C_{A,B}$ characterizing deviation of the dispersion relation $E(k)$ from its parabolic form, which yielded an acceptable agreement of the calculated and experimental temperature dependences for the kinetic coefficients in this material. It was found that $C_{A,B} = k_{A,B}(E_0 - E_g)$ for p-$CuInSe_2$ and their $A^{II}B^{VI}$ analogs, allowing to refine the values of C_A for CdSe and CdS. We also obtained a phenomenological expression (15) for the coefficients $A_{\perp,\parallel}$ in formula (13) describing the spectral dependence of light absorption tensor close to the fundamental absorption edge as a function of E_g. Moreover, the dependence $\left(A_{\parallel}^* / A_{\perp}^* - A_{\parallel}^*(0) / A_{\perp}^*(0)\right) \cdot 100\% = f(C_1)$ proved to be linear in the first approximation for CdSe, CdS, ZnO and $CuInSe_2$ with wurtzite and chalcopyrite structure; the experimental data known for p-$CuInSe_2$ fits reasonably our theoretical calculations performed for the components of the effective masses given by the formula (10).

The obtained effective mass values make it possible to properly explain the component anisotropy for the interband light absorption tensor, as well as the experimental data on temperature dependence of the kinetic coefficients within p-$CuInSe_2$ in the temperature range 100 – 350 K.

References

1. H.W. Schock, Solar cells based on $CuInSe_2$ and related compounds: recent progress in Europe // *Sol. Energy Mater*. **34**, p. 19-26 (1994).

2. U. Rau, H.W. Schock, Electronic properties of Cu(In, Ga)Se_2 heterojunction solar cells-recent achievements, current understanding, and future challenges // *Appl. Phys. A* **69**, p. 131-147 (1999).

3. J.E. Jaffe, A. Zunger, Electronic structure of the ternary chalcopyrite semiconductors // *Phys. Rev B* **28**, p. 5822-5846 (1983).

4. J.E. Jaffe, A. Zunger, Theory of band-gap anomaly in ABC_2 chalcopyrite semiconductors // *Phys. Rev. B* **29**, p. 1882-1906 (1984).

5. H.T. Shaban, M. Mobarak, M.M. Nassary, Characterization of $CuInSe_2$ single crystal // *Physica B* **389**, p. 351-354 (2007).

6. V.A. Chaldyshev, G.F. Karavaev, To a question about energy spectra structure in chalcopyrite crystals // *News of the High Education Institutions* **2**, p. 28-30 (1964).

7. G.F. Karavaev, A.S. Poplavnoy, Investigation of the energy spectra for the electrons in semiconductor compounds with chalcopyrite lattice using a perturbation theory // *Fizika tverdogo tela* **8**, p. 2144-2148 (1966) (in Russian).

8. H. Neumann, W. Kissinger, H. Sobotta, V. Riede, G. Kühn, Hole effective masses in $CuInSe_2$ // *Phys. status solidi* (*b*) **108** (2), p. 483-487 (2006).

9. P.M. Gorley, O.O. Galochkina, Yu.V. Vorobiev, J. González-Hernández, Temperature dependence of kinetic coefficients and thermal voltage for p-$CuInSe_2$ crystals // *Thermoelectric* **2**, p. 48-56 (2008).

10. P.P. Horley, V.V. Gorley, P.M. Gorley, J. Gonzalez-Hernandez, Yu.V. Vorobiev, On correlation of CdS and CdSe valence band parameters // *Thin Solid Films* **480-481**, p. 373-376 (2005).

11. E. Gutsche, E. Jahne, Spin-orbit splitting of the valence band of wurtzite type crystals // *Phys. status solidi* (*b*) **19**, p. 823-832 (1967).

12. E. Jahne, E. Gutsche, Valence band structure of wurtzite type crystals // *Phys. status solidi* **21**, p. 57-68 (1967).

13. K. Yoodee, J.C. Woolley, V. Sa-yakanit, Effects of p-d hybridization on the valence band of I-III-VI_2 chalcopyrite semiconductors // *Phys. Rev. B* **30** (10), p. 5904-5915 (1984).

14. W.R.L. Lambrecht, A.V. Rodina, S. Limpijumnong, D. Segall, B.K. Meyer, Valence-band ordering and magneto-optic exciton fine structure in ZnO // *Phys. Rev. B* **65**, 075207-1-075207-12 (2002).

15. L.C. Lew Yan Voon, M. Willatzen, M. Cardona, N.E. Christencen, Terms linear in k in the band structure of wurtzite-type semiconductors // *Phys. Rev. B* **53**(16), p. 10703-10714 (1996).

16. E.I. Rashba, Symmetry of the energy bands in wurtzite crystals // *Fizika tverdogo tela* **1**(3), p. 407-421 (1959) (in Russian).

17. M. Cardona, Band parameters of semiconductors with zincblende, wurtzite, and germanium structure // *J. Phys. Chem. Solids* **24**, p. 1543-1555 (1963).

18. J.L. Shay, B. Tell, H.M. Kasper, L.M. Schiavone, Electronic structure of $AgInSe_2$ and $CuInSe_2$ // *Phys. Rev. B* **7**, p. 4485-4490 (1973).

19. A. Continenza, R.M. Wentzcovitch, A.J. Freeman, Theoretical investigation of graphitic BeO // *Phys. Rev. B* **41**(6), p. 3540-3544 (1990).

20. T.S. Moss, G.J. Burrell, B. Ellis, *Semiconductor Opto-Electronics*. Mir Publ., Moscow, 1976 (in Russian).

21. P.M. Gorley, V.V. Khomyak, Yu.V. Vorobiev, J. Gonzalez-Hernandez, P.P. Horley, O.O. Galochkina, Electron properties of n- and p-$CuInSe_2$ // *Solar Energy* **82**, p. 100-105 (2008).

22. C. Rincon, R. Marquez, Defect physics of the $CuInSe_2$ chalcopyrite semiconductors // *J. Phys. Chem. Solids* **60**, p. 1865-1873 (1999).

23. H. Neumann, R.D. Tomlinson, Band-gap narrowing in n-type $CuInSe_2$ single crystals // *Solid State Communs* **57**, p. 591-594 (1986).

24. I. Hernandez-Calderon, Optical properties and electronic structure of wide band gap II-VI semiconductors, Chap. 4, In: *II-VI Semiconductor Materials and their Applications*, Eds. M.C. Tamargo. Taylor and Francis, New York, 2002, p. 113-170.

25. J.D. Park, B.H. Chang, I.H. Choi, Thermoelectric power of p-$CuInSe_2$ single crystals // *J. Korean Phys. Soc.* **22**, p. 113-213 (1989).

26. M.I. Alonso, K. Wakita, J. Pascual, M.Garriga, N. Yamamoto, Optical functions and electronic structure of $CuInSe_2$, $CuGaSe_2$, $CuInS_2$ and $CuGaS_2$ // *Phys. Rev. B* **63**, 075203-1-075203-13 (2001).

27. T. Irie, S. Endo, S. Kimura, Electrical properties of p- and n-type $CuInSe_2$ single crystals // *Jpn J. Appl. Phys.* **18**, p. 1303-1310 (1979).

28. O. Madelung, U. Rössler, M. Schulz, Zinc oxide (ZnO) electron effective masses, **41B**, In: *II-VI and I-VII Compounds; Semimagnetic Compounds*. Springer-Verlag, 2006.

29. J.L. Shay, E. Buehler, Electroreflectance study of the energy-band structure of $CdSnP_2$ // *Phys. Rev. B* **2**(10), p. 4104-4109 (1970).

30. J.E. Rowe, J.L. Shay, Extension of the quasi-cubic model to ternary chalcopyrite crystals // *Phys. Rev. B* **3**(2), p. 451-453 (1971).